

CHEMISTRY

AN **ASIAN** JOURNAL

www.chemasianj.org

Accepted Article

Title: β -Cyclodextrin functionalized nanoporous graphene oxides for efficient resolution of asparagine enantiomers

Authors: Fengxiang Qie, Jiahui Guo, Bin Tu, Xing Zhao, Yuchun Zhang, and Yong Yan

This manuscript has been accepted after peer review and appears as an Accepted Article online prior to editing, proofing, and formal publication of the final Version of Record (VoR). This work is currently citable by using the Digital Object Identifier (DOI) given below. The VoR will be published online in Early View as soon as possible and may be different to this Accepted Article as a result of editing. Readers should obtain the VoR from the journal website shown below when it is published to ensure accuracy of information. The authors are responsible for the content of this Accepted Article.

To be cited as: *Chem. Asian J.* 10.1002/asia.201800970

Link to VoR: <http://dx.doi.org/10.1002/asia.201800970>

A Journal of



A sister journal of *Angewandte Chemie*
and *Chemistry – A European Journal*

WILEY-VCH

β -Cyclodextrin functionalized nanoporous graphene oxides for efficient resolution of asparagine enantiomers

Fengxiang Qie^{a,§}, Jiahui Guo^{a,b,§}, Bin Tu^{a,§}, Xing Zhao^a, Yuchun Zhang^a, and Yong Yan^{a,*}

^aCAS Key Laboratory of Nanosystem and Hierarchical Fabrication, CAS Center for Excellence in Nanoscience, National Center for Nanoscience and Technology, Beijing 100190, China

^bUniversity of Chinese Academy of Sciences, Beijing, 100049, China

[§]These authors contributed equally to this work

*Correspondence to: yany@nanoctr.cn

Efficient resolution of racemic mixture has long been the most attractive but challenging subject since Pasteur separated tartrate enantiomers in 19th century. Graphene oxide (GO) could be flexibly functionalized by using a variety of chiral host molecules and therefore, was expected to show excellent enantioselective resolution performance. However, this combination with efficient enantioselective resolution capability has been scarcely demonstrated. Here, Nanopores graphene oxides were firstly produced and then covalently functionalized by using a chiral host material— β -cyclodextrin (β -CD). This chiral GO displayed enantioselective affinity toward the *L*-enantiomers of amino acids. Particularly, > 99% of *L*-asparagine (Asn) was captured in a racemic solution of Asn while the adsorption of *D*-enantiomer was not observed. This remarkable resolution performance was subsequently modelled by using an attach-pull-release dynamic method. We expect this preliminary concept could be expanded to other chiral host molecules and be employed to current membrane separation technologies and finally show practical use for many other racemates.

The two enantiomers of chiral molecule are non-superimposable mirror images but have almost the same chemical and/or physical properties and therefore, are usually hard to separate.^[1] However, enantioselective resolution of these two enantiomers is of particular importance because distinct biological and/or pharmacological effects were commonly found in chiral biomolecules and pharmaceuticals.^[2] Many enantioselective resolution techniques including chromatography, crystallization, and membrane-based separations such as chiral membranes and/or molecularly imprinted membranes have been developed.^[3] Although these techniques exhibit various advantages, they still face important technical limitations, such as high energy consumption, high cost, low efficiency, discontinuous operation, and difficult to scale-up.^[4] On the other hand, graphene oxide contains plenty of reactive oxygen groups (-COOH, -OH, carbonyl, and epoxy), which provides possibility for chemical modification and produces functional materials for a wide range of applications.^[5] In particular, these GOs have been demonstrated to efficiently separate various materials such as cations,^[6] gases,^[7] and organic molecules^[8] because of their properties such as large surface area, tunable interactive sites, as well as adjustable interlayer spacing.^[9]

Chiral molecules, including polymers^[10] and biomolecules,^[11] have also been utilized to functionalize these graphene oxides and show typical enantioselective interaction toward guest enantiomers.^[12] In this way, chiral GO enantioselective sensors were demonstrated.^[13] However, this general recognition phenomenon has been rarely applied to separate enantiomers or racemates because of great challenges in fabricating chiral GOs with efficient enantioselective resolution capabilities.^[14] This low efficiency

is probably due to insufficient chiral host molecules and mismatch between chiral host and guest pairs.^[15] Moreover, instead of investigating the “response/signal” difference between pure *D*- and *L*-enantiomers in these chiral sensors, separating one enantiomer from a mixture of racemic enantiomers is of particular difficult because of fierce competition between the two enantiomers.^[16] Furthermore, sites for molecular interaction is also important for the host-guest recognition. Ariga *et al* conducted a systematic investigation of a great variety of combinations of the host monolayers and aqueous guests where the molecular recognition is performed at the air-water interface.^[17] Here, our method is, therefore, covalently bonding nanoporous GOs with chiral host materials as much as possible and performing the host-guest molecular recognition in aqueous solution. Meanwhile, we choose a classic host-guest pair of β -CD and racemic amino acid solutions where enantioselective interaction was found for many other systems but seldom for GOs.^[18]

Figure 1a shows a schematic illustration of enantioselective resolution of amino acids by using chiral graphene oxide. β -CDs as chiral host molecules were covalently connected on GO through an amidation reaction between -COOH and -NH₂ groups. To increase the density of chiral host molecules, nanopores in GO were created. This nanoporous chiral GOs could selectively bind the *L*-enantiomers in an amino acid racemates solution. The *D*-enantiomers were then collected by isolating these GOs with simple centrifuging or filtrating process. Here, five amino acid racemates were mixed with nanoporous chiral GOs and apparent enantioselective resolution phenomenon has been observed (Figure 1b, HPLC results). Specifically, the ratio of *L*-enantiomer for all

five amino acids was lower than 50%, which indicated that these *L*-enantiomers were selectively adsorbed. In addition, more than 99% of *L*-Asn was captured by these chiral GOs, leaving almost enantiopure *D*-Asn solution. This surprising efficient resolution capability (~99% enantiomeric excess, *ee*) was hard to achieve especially for those using chiral graphene oxides.

To synthesize these nanoporous chiral GOs, commercial graphene oxides (Figure 2a, no apparent nanopores) were firstly oxidized by using nitric acid due to the relatively higher chemical activities intrinsically associated with the defect sites of GOs (see details in the Supporting information). This produced nanoporous GO (N-GO) where the density of –COOH group has increased and reached the maximum value at *ca.* 4 hrs oxidation (Figure 2d, statistics and S1, XPS data). Specifically, ~30% more –COOH groups were produced and its ratio increased to ~10%. Further oxidation led to a decrease of –COOH density which is probably because as the increase of nanopore diameter, the effective surface area and total edge length have reduced. These nanoporous structures were confirmed by comparing the TEM images where these 4~5 nm nanopores (Figure 2c, 4 hrs oxidation, the inset show the distribution of nanopores) were gradually expanded to *ca.* 80 nm nanopores (Figure S2, 10 hrs oxidation). The pore size distribution and surface area of N-GO were subsequently investigated by using TEM and nitrogen adsorption-desorption isotherms (Figure S3 and S4, Table S1, see details in the Supporting information). On the other hand, it must emphasize that these nanoporous GOs could be readily dispersed and stabilized in aqueous solution for more than one year (Figure 1b photographs, *ca.* 1 mg·mL⁻¹). This indicated that these

nanoporous GOs might be monodispersed and was then confirmed by AFM result (Figure S5). We believe this monodisperse characteristic is beneficial for the performance of following resolution performance because any agglomeration would reduce the effective density of active sites (-COOH) and subsequent chiral host molecules.

Next, chiral host molecules (β -CD) were then covalently bonded onto these nanoporous GOs by using the EDC/NHS method.^[19] The feed ratio between β -CD and GO was determined by recording the changes of the zeta potential because of their distinct surface charge characteristics (Figure 2e, green and orange histograms). As more host molecules bonded, the Zeta potential of the complex gradually decreased and finally stabilized at a steady value (Figure 2e, blue histograms), which indicated that the majority of -COOH was transformed into -CONH- groups. This amidation reaction was further confirmed by carrying out FTIR and XPS spectra measurements. The FTIR spectra of β -CDs, nanoporous GOs, and their complex were shown and compared in Figure 2f. The nanoporous GOs displayed characteristic stretching vibrational modes at 1730, 1625, 1216, and 1039 cm^{-1} , corresponding to C=O (carbonyl), C=C (aromatic), C-OH (hydroxyl), and C-O (epoxy) respectively (Figure 2f, orange curve).^[20] After functionalization (Figure 2f, blue curve), the stretching band of the amide C-N (1240 cm^{-1}), a sharp stretching vibration of -CH₂ (2930 cm^{-1}), as well as typical features of glucose units and glucose rings (500-1200 cm^{-1}) were appeared in these nanoporous chiral GOs.^[21] Moreover, the characteristic peaks of amide group were also found in these complex where a broad peak at 1605 cm^{-1} was due to bending vibration of N-H

group and a band at 1660 cm^{-1} corresponded to the stretching of C=O groups.^[22] The XPS spectra of nanoporous GOs before and after functionalization were subsequently recorded (Figure 2g). C-N (399.7 eV) and N-H (401.7 eV) peaks were observed in these functionalized GOs while no apparent peak was found for nanoporous GOs (Figure 2g, orange curve).^[22-23]

The amount of connected β -CD on these N-GOs was subsequently quantified by using thermogravimetric analysis. As shown in Figure S6, β -CD-nanoporous-GOs show a 3.6% weight loss below $120\text{ }^{\circ}\text{C}$ as a result of the release of absorbed water, and a further rapid weight loss (13.1%) from 140 to $250\text{ }^{\circ}\text{C}$ which is attributed to the removal of the oxygen-containing functional groups. Comparing to non-functionalized nanoporous GOs, β -CD-nanoporous-GOs displayed a sharp drop in the range of 250 - $340\text{ }^{\circ}\text{C}$, with a mass loss of 23.1 wt%, should be attributed to the decomposition of β -CD moieties, which is consistent with the thermal decomposition profile of pure β -CDs.

These nanoporous chiral GOs were then applied for resolving amino acid enantiomers. In a racemic mixture solution, chiral GOs were added to capture the enantiomers and then isolated. It was found that excess *D*-enantiomers of asparagine were left in the solution where a negative peak at *ca.* 200 nm appeared in the circular dichroism spectrum (Figure 3a). This indicated that the nanoporous chiral GOs selectively captured *L*-Asn and the host-guest interaction between *L*-Asn and GOs was stronger comparing to the other one. In addition, more *D*-enantiomers were collected as the increase of incubation time (Figure 3a, and b, red square left y-axis). This was further confirmed by using HPLC measurements. As the increase of interaction time,

the peak of *L*-Asn gradually decreased and finally disappeared while no apparent changes have been observed for *D*-Asn (Figure 3c, and b, black triangle and blue circle, right y-axis). Specifically, more than 99% of *L*-Asn was adsorbed by chiral GOs and almost enantiopure *D*-Asn was obtained.

Four additional amino acids, phenylalanine (Phe), tryptophan (Trp), leucine (Leu), and histidine (His) were subsequently tested. Similarly, *L*-enantiomers of these acids were also captured by nanoporous chiral GOs, but the enantiomeric excess values were much lower comparing to asparagine (Figure 1b, S9). Such an efficient resolution capability (~99% *ee*) toward Asn enantiomers was scarcely found and we believe both nanoporous GOs and β -CD-Asn host-guest pair were indispensable. Nanoporous structures provided sufficient chiral host sites while the specific but not strong host-guest interactions guaranteed enantioselectivity.

The enantioselective resolution capabilities of these chiral GOs were then evaluated by using an attach-pull-release dynamic model.^[24] In this model, enantiomers were forced to penetrate through the cavity of β -CD in four steps, specifically, bound step, attached step, pulled step, and unbound step (Figure 4a-d). In these steps, 60 consecutive interaction sites were calculated. At each site, the enantiomers were allowed to stay for *ca.* 2.5 ns which is enough to find their most stable conformation. The magnitude of applied force and corresponding work were determined by the non-covalently weak interactions (*e.g.* H-bonding, Van der Waals force) between the host and two enantiomeric guest molecules. Finally, the overall binding free energies were calculated from $\Delta G_{bind}^o = -(W_{attach} + W_{pull} + W_{release-conf} + W_{release-std})$

equation.^[24] Here, the free energies of both asparagine and tryptophan were calculated and compared. For Asn, the binding energies of *L*- and *D*-enantiomers were -6.78 kcal·mol⁻¹ and -6.36 kcal·mol⁻¹ respectively which were much lower than Trps (*L*-Trp, -11.29 kcal·mol⁻¹ and *D*-Trp -11.28 kcal·mol⁻¹). This indicated that the host-guest interaction between Trp and β -CD was much stronger where a higher binding constant was calculated by using $K_{bind} = \exp(\Delta G_{bind}^0/RT)$ equation (*ca.* 1.9E8).

However, the enantioselective resolution performance should be determined by the binding energy difference between two enantiomers rather than absolute binding energy between host and guest molecules. The energy differences of two enantiomers of asparagine and tryptophan were calculated as 0.42 kcal·mol⁻¹ and 0.01 kcal·mol⁻¹ respectively (Figure 4e, blue histograms, left y-axis). In this way, Asn with lower binding constant should display stronger enantioselective resolution capability than Trp which agreed well with experimental observations (Figure 1b). The binding constant ratios (K_L/K_D) between two enantiomers were also calculated. This ratio for Asn was *ca.* 2 while for Trp was very close to 1 (Figure 4e, orange histograms, right y-axis), further confirmed that these chiral molecules displayed stronger enantioselective resolution capability toward asparagines.

Next, we inferred that the main reasons for the stronger interactions between *L*-asparagines and β -CD-nanoporous-GOs are attributed to 1) The structures---the dominant interaction between amino acids (tryptophan, phenylalanine, histidine) and β -CD-nanoporous-GOs is the π - π interaction. While for leucine and asparagine, the main interaction with β -CD-nanoporous-GOs is hydrogen bonding interaction.

Comparing to π - π interaction ($\sim 10 \text{ KJ.mol}^{-1}$), hydrogen bonding ($\sim 25\text{-}40 \text{ KJ.mol}^{-1}$) possesses a higher binding energy. Besides, asparagine has more interaction sites for hydrogen bonding. 2) The chiral selectivity is dependent on the β -CD which is in favor of *L*- over *D*-type.

Finally, it is important to compare the recognition efficiency of our β -CD-nanoporous-GOs with other GO-based techniques. Deng has synthesized chiral 3D porous hybrid foams by using optically active helical-substituted polyacetylene and reduced graphene oxide (RGO). This foam was used as additive to induce enantioselective crystallization of racemic alanine. The *ee* reached the maximum value (88%) at third cycle with 96 hrs interaction.^[25] Hong et al developed a novel GO-modified affinity capillary monoliths by employing human serum albumin (HSA) or pepsin as chiral selector. Amino acid enantiomers were chosen as the model analytes and the resolution (*R_s*) and separation factor ($\alpha \sim 1.2$) are used to evaluate the chiral separation capability.^[11b] Meng et al fabricated graphene-based chiral membranes and the enantioseparation performance toward 3, 4-Dihydroxy-*D* or *L*-phenylalanine were studied. Notable separation factor ($\alpha \sim 1.25$) was achieved even at flux as high as $250 \text{ nmoles}\cdot\text{cm}^{-1}\cdot\text{h}^{-1}$.^[12a] With different evaluating parameters, it is hard to compare the enantioseparation performance of these GO-based chiral materials. However, in the context of *ee*, our method is competitive where 99% *ee* has observed for asparagine enantiomers.

To conclude, we have produced a new type of nanoporous chiral graphene oxides. These chiral GOs show efficient enantioselective resolution capability toward

asparagines. A molecular dynamic model was proposed to explain these observations. Looking forward, we wish these nanoporous chiral GOs could be combined with current membrane and/or column chromatography (as stationary phase materials) separation technologies and show real application in resolving important chiral materials such as pharmaceutical intermediates, agrochemicals, and fragrances.^[26]

Supplementary information

Electronic supplementary information (ESI) available: Materials and methods, Theoretical details, and additional figures.

Conflicts of interest

There are no conflicts to declare.

Acknowledgements

This work was supported by the Ministry of Science and Technology of China (No 2016YFA0203400) and the Chinese Academy of Sciences.

References

- [1] G. Subramanian, *Chiral Separation Techniques: A Practical Approach*, Wiley-VCH Verlag GmbH & Co. KGaA, Weinheim, Germany, **2006**, p.
- [2] a) S. Ahuja, *Chirality of Biomolecules and Biotechnology Products*, John Wiley & Sons, Inc., Hoboken, New Jersey, **2011**, p; b) F. Jamali, R. Mehvar and F. M. Pasutto, *J. Pharm. Sci.* **1989**, *78*, 695-715.
- [3] a) T. J. Ward and K. D. Ward, *Anal. Chem.* **2012**, *84*, 626-635; b) W. H. Pirkle and T. C. Pochapsky, *Chem. Rev.* **1989**, *89*, 347-362; c) A. Svang-Ariyaskul, W. J. Koros and R. W. Rousseau, *Chem. Eng. Sci.* **2009**, *64*, 1980-1984; d) R. Xie, L.-Y. Chu and J.-G. Deng, *Chem. Soc. Rev.* **2008**, *37*, 1243-1263; e) M. Ulbricht, *J. Chromatogr. B* **2004**, *804*, 113-125.
- [4] N. M. Maier, P. Franco and W. Lindner, *J. Chromatogr. A* **2001**, *906*, 3-33.
- [5] a) Y. Zhu, S. Murali, W. Cai, X. Li, J. W. Suk, J. R. Potts and R. S. Ruoff, *Adv. Mater.* **2010**, *22*, 3906-3924; b) V. Georgakilas, J. N. Tiwari, K. C. Kemp, J. A. Perman, A. B. Bourlinos, K. S. Kim and R. Zboril, *Chem. Rev.* **2016**, *116*, 5464-5519.

- [6] A. Esfandiari, B. Radha, F. C. Wang, Q. Yang, S. Hu, S. Garaj, R. R. Nair, A. K. Geim and K. Gopinadhan, *Science* **2017**, *358*, 511-513.
- [7] H. W. Kim, H. W. Yoon, S.-M. Yoon, B. M. Yoo, B. K. Ahn, Y. H. Cho, H. J. Shin, H. Yang, U. Paik, S. Kwon, J.-Y. Choi and H. B. Park, *Science* **2013**, *342*, 91-95.
- [8] A. Morelos-Gomez, R. Cruz-Silva, H. Muramatsu, J. Ortiz-Medina, T. Araki, T. Fukuyo, S. Tejima, K. Takeuchi, T. Hayashi and M. Terrones, *Nat. Nanotechnol.* **2017**, *12*, 1083-1088.
- [9] L. Chen, G. Shi, J. Shen, B. Peng, B. Zhang, Y. Wang, F. Bian, J. Wang, D. Li and Z. Qian, *Nature* **2017**, *550*, 380-383.
- [10] W. Li, B. Wang, W. Yang and J. Deng, *Macromol. Rapid Commun.* **2015**, *36*, 319-326.
- [11] a) A. W. Hauser, N. Mardirossian, J. A. Panetier, M. Head-Gordon, A. T. Bell and P. Schwerdtfeger, *Angew. Chem. Int. Ed.* **2014**, *53*, 9957-9960; b) T. Hong, X. Chen, Y. Xu, X. Cui, R. Bai, C. Jin, R. Li and Y. Ji, *J. Chromatogr. A* **2016**, *1456*, 249-256.
- [12] a) C. Meng, Y. Sheng, Q. Chen, H. Tan and H. Liu, *J. Membr. Sci.* **2017**, *526*, 25-31; b) I. Fuchs, N. Fechner, M. Antonietti and Y. Mastai, *Angew. Chem. Int. Ed.* **2016**, *55*, 408-412.
- [13] a) E. Zor, I. H. Patir, H. Bingol and M. Ersoz, *Biosens. Bioelectron.* **2013**, *42*, 321-325; b) W. Wei, K. Qu, J. Ren and X. Qu, *Chem. Sci.* **2011**, *2*, 2050-2056; c) Q. Han, Y. Wang, Y. Huang, L. Guo and Y. Fu, *Analyst* **2013**, *138*, 2051-2056; d) E. Zor, M. Esad Saglam, S. Alpaydin and H. Bingol, *Analytical Methods* **2014**, *6*, 6522-6530; e) S. Ates, E. Zor, I. Akin, H. Bingol, S. Alpaydin and E. G. Akgemci, *Analytica Chimica Acta* **2017**, *970*, 30-37; f) X. Mao and H. Li, *Journal of Materials Chemistry B* **2013**, *1*, 4267-4272; g) J. Ou, Y. Zhu, Y. Kong and J. Ma, *Electrochemistry Communications* **2015**, *60*, 60-63; h) Y.-f. Hu, Z.-h. Zhang, H.-b. Zhang, L.-j. Luo and S.-z. Yao, *Talanta* **2011**, *84*, 305-313; i) X. Juanjuan, W. Qinghong, X. Chunzhi, X. Qiao, L. Xia and F. Yingzi, *Electroanalysis* **2016**, *28*, 868-873; j) Y. Tao, J. Dai, Y. Kong and Y. Sha, *Analytical Chemistry* **2014**, *86*, 2633-2639.
- [14] Y. Xiao, H.-Q. Wang, H. Zhang, Z.-Q. Jiang, Y.-Q. Wang, H. Li, J. Yin, Y.-Y. Zhu and Z.-Q. Wu, *Polym. Sci. A* **2017**, *55*, 2092-2103.
- [15] a) B. Kesanli and W. B. Lin, *Coord. Chem. Rev.* **2003**, *246*, 305-326; b) T. H. Webb and C. S. Wilcox, *Chem. Soc. Rev.* **1993**, *22*, 383-395.
- [16] a) H. J. Federsel in *2.17 - Chiral Drug Discovery and Development – From Concept Stage to Market Launch A2 - Taylor, John B.* (Ed. D. J. Triggle), Elsevier, Oxford, **2007**, pp. 713-736; b) X. Lin, R. Gong, J. Li, P. Li, J. Yu and A. E. Rodrigues, *Journal of Chromatography A* **2016**, *1467*, 347-355.
- [17] a) K. Ariga, T. Michinobu, T. Nakanishi and J. P. Hill, *Curr. Opin. Colloid Interface Sci.* **2008**, *13*, 23-30; b) T. Michinobu, S. Shinoda, T. Nakanishi, J. P. Hill, K. Fujii, T. N. Player, H. Tsukube and K. Ariga, *J. Am. Chem. Soc.* **2006**, *128*, 14478-14479; c) K. Ariga, G. J. Richards, S. Ishihara, H. Izawa and J. P. Hill, *Sensors* **2010**, *10*, 6796-6820.
- [18] R.-P. Liang, C.-M. Liu, X.-Y. Meng, J.-W. Wang and J.-D. Qiu, *Journal of Chromatography A* **2012**, *1266*, 95-102.

- [19] N. Suzuki, Y. Wang, P. Elvati, Z. B. Qu, K. Kim, S. Jiang, E. Baumeister, J. Lee, B. Yeom, J. H. Bahng, J. Lee, A. Violi and N. A. Kotov, *Acs Nano* **2016**, *10*, 1744-1755.
- [20] X. T. Zheng and C. M. Li, *Molecular Pharmaceutics* **2012**, *9*, 615-621.
- [21] W. Feng, C. Liu, S. Lu, C. Zhang, X. Zhu, Y. Liang and J. Nan, *Microchim. Acta* **2014**, *181*, 501-509.
- [22] I. Kaminska, M. R. Das, Y. Coffinier, J. Niedziolka-Jonsson, J. Sobczak, P. Woisel, J. Lyskawa, M. Opallo, R. Boukherroub and S. Szunerits, *ACS Appl. Mater. Interfaces* **2012**, *4*, 1016-1020.
- [23] H. J. Kim, I.-S. Bae, S.-J. Cho, J.-H. Boo, B.-C. Lee, J. Heo, I. Chung and B. Hong, *Nanoscale Res. Lett.* **2012**, *7*, 1-7.
- [24] N. M. Henriksen, A. T. Fenley and M. K. Gilson, *J. Chem. Theory Comput.* **2015**, *11*, 4377-4394.
- [25] B. Wang, W. Li and J. Deng, *J. Mater. Sci.* **2017**, *52*, 4575-4586.
- [26] E. Sanganyado, Z. Lu, Q. Fu, D. Schlenk and J. Gan, *Water Research* **2017**, *124*, 527-542.

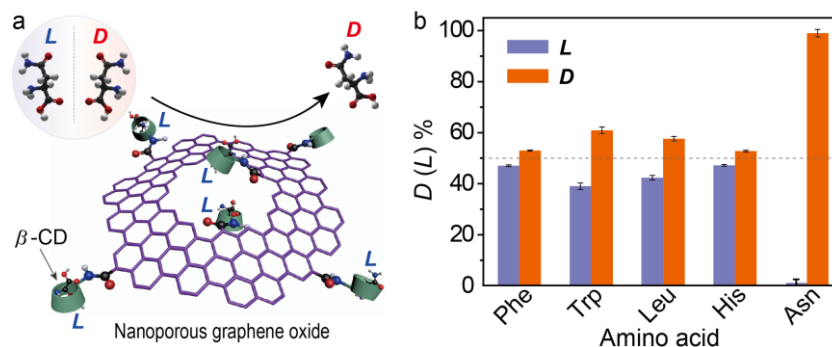


Figure 1. (a) The scheme of enantioselective resolution by using nanoporous chiral graphene oxides. β -CDs were covalently bonded on nanoporous GO and selectively bound the L -enantiomers in amino acid racemic solution. (b) Resolution capability of nanoporous chiral GO ($0.8 \text{ mg}\cdot\text{mL}^{-1}$) toward five amino acid racemates (3 mM), specifically, phenylalanine (Phe), tryptophan (Trp), leucine (Leu), histidine (His), and asparagine (Asn). The nanoporous chiral GO selectively bound the L -enantiomer for all five amino acids and displayed the best performance toward Asn racemates ($D\text{-Asn}\% > 99\%$). Note: 1) The ratio is calculated by comparing the HPLC peak area of D - and L -enantiomers. 2) The error bar is based on four independent experiments. 3) The upper solution is used for HPLC experiment (see details in experimental section) and therefore, the ratio of L -enantiomer is less than D -enantiomer indicates that the nanoporous GO selectively binds L -enantiomer.

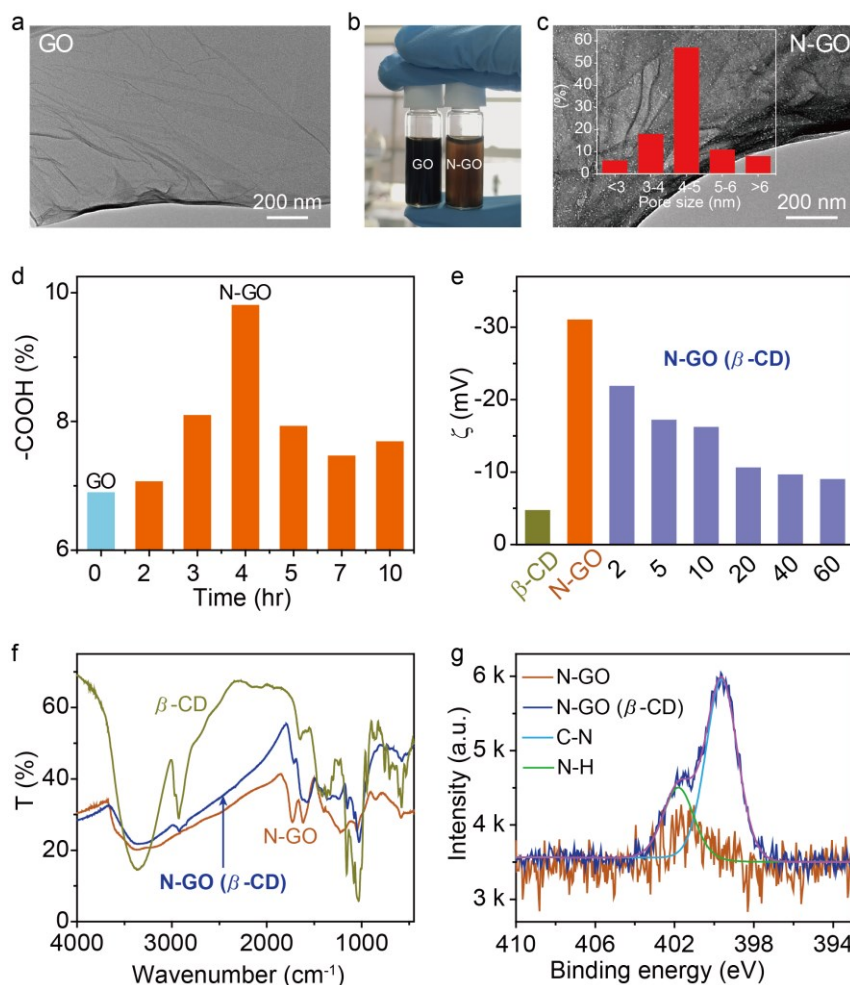


Figure 2. Synthesis of nanoporous graphene oxides (N-GO) and functionalization of these GOs by using β -CDs. TEM images and photographs of the aqueous dispersions of commercial GO (a, b-left) and nanoporous GO (oxidation for 4 hrs, c, b-right). The concentration of nanoporous GO is *ca.* 1 mg·mL⁻¹. Nanopores (*ca.* 4~5 nm in diameter) were created and more -COOH groups were produced on GOs. (d) The ratios of -COOH group on GOs oxidized for different time (calculated from XPS data). (e) to (g) Zeta potential, FTIR spectra, and N1s XPS spectra of nanoporous GOs before and after functionalization. The zeta potential was monitored by changing the feed ratio between β -CD and GO (0.8 mg·mL⁻¹). The feed ratio is then fixed at 40 for FTIR, XPS and the following resolution experiment.

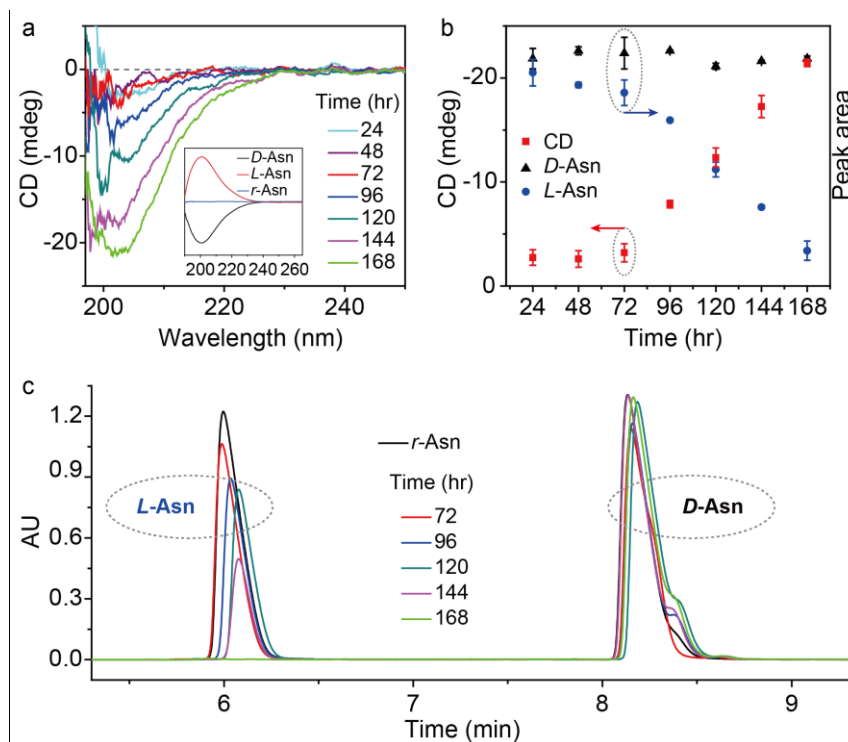


Figure 3. Enantioselective resolution of Asn. **(a)** The circular dichroism spectra of the upper solution after enantioselective interaction between nanoporous chiral GOs and Asn racemates for different time. The inset shows the spectra of enantiopure *D*-Asn, *L*-Asn, and *r*-Asn, which indicated that *D*-Asn was accumulating in the upper solution while *L*-Asn was gradually adsorbed by nanoporous chiral GOs. **(b)** The statistics of circular dichroism intensity (red square, left y axis) and HPLC peak area (*D*-Asn and *L*-Asn, black triangle and blue circle, right y axis) of the upper solution. The error bar is based on four independent experiments. **(c)** Typical HPLC result of the upper solution at different time.

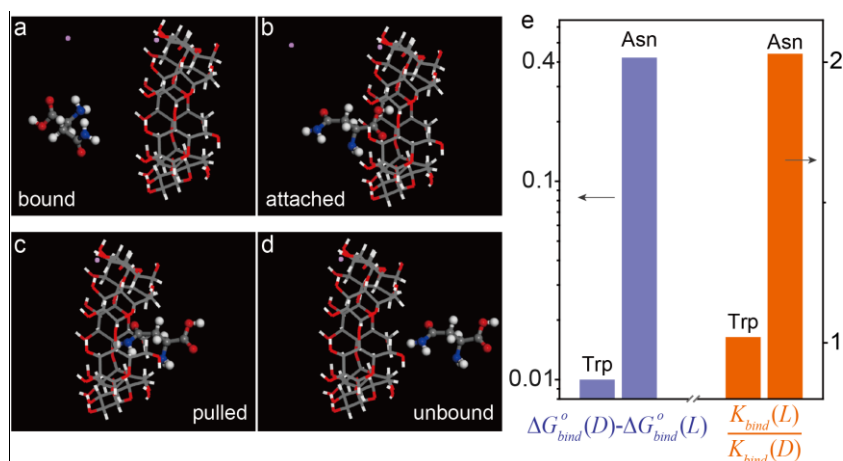


Figure 4. (a) to (d) The enantioselective interaction between β -CD and amino acids was modelled by using an attach-pull-release method. The enantiomers were forced to penetrate through the cavity of β -CD and the overall binding energies were calculated. (e) The difference of binding energy (blue histogram, left y axis) and corresponding binding constant ratio (orange histogram, right y axis) between *D*- and *L*-enantiomer of Trp and Asn.